LBL-16539

Lawrence Berkeley Laboratory

UNIVERSITY OF CALIFORNIA

Accelerator & Fusion Research Division

Presented at the 12th International Conference on High-Energy Accelerators, Fermi National Accelerator Laboratory, Batavia, IL, August 11-16, 1983

A PRELIMINARY STUDY OF MAGNET DESIGN FOR AN SSC

C.E. Taylor and R.B. Meuser

August 1983

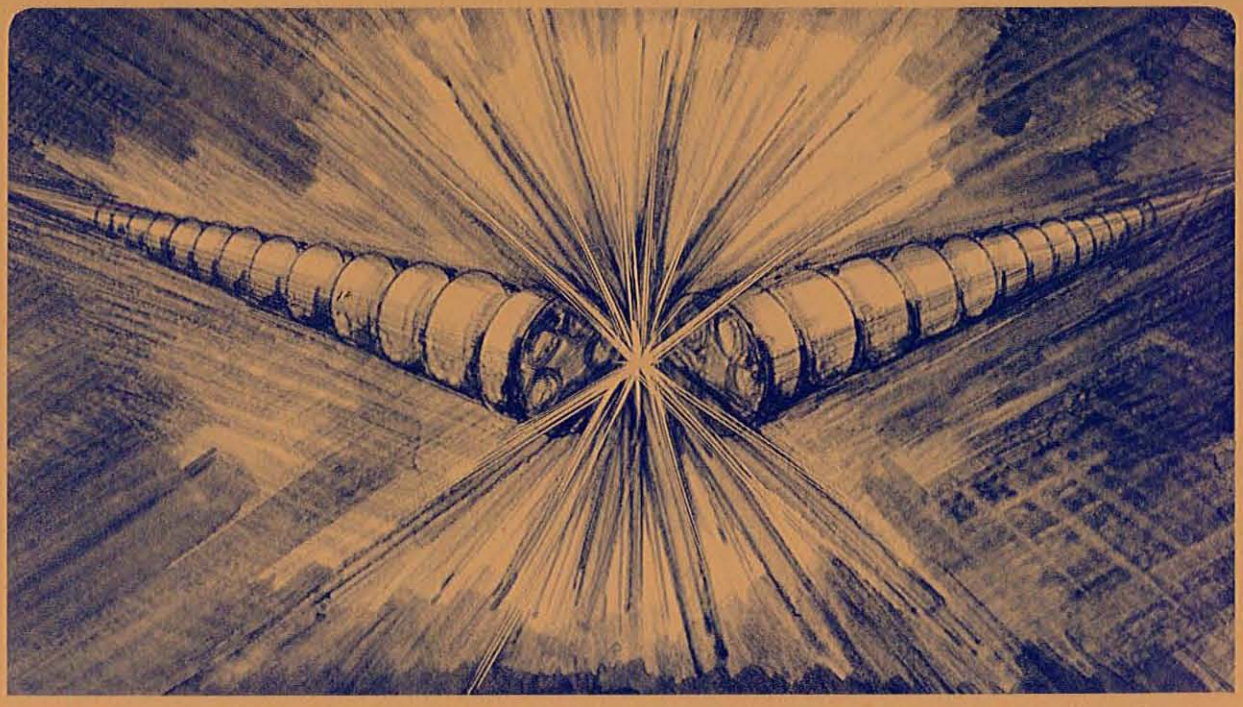

Prepared for the U.S. Department of Energy under Contract DE-AC03-76SF00098

A PRELIMINARY STUDY OF MAGNET DESIGN FOR AN SSC*

C.E. Taylor and R.B. Meuser
Lawrence Berkeley Laboratory, University of California, Berkeley, California 94720

Introduction

The overriding design consideration for the SSC magnets is that cost of the facility be minimized; at 8 T, approximately 40 km of bending magnets is required for each ring of a 20 TeV collider. To accomplish this, we choose the following general guidelines for our preliminary study:

- Both rings are located in the same cryostat; i.e., a "two-in-one" design.
- The bore diameter is as small as possible, perhaps less than 50 mm.
- Superconductor current density is as high as possible, within the limits of what can be expected from industry within the next two or three years.

The two-in-one design was considered as a cost-saving option for the CBA,[1] but was not adopted as the preferred design because to do so might have required more development time; moreover, sufficient refrigeration capacity for two separate rings had already been purchased, thus potential cost saving was minimal. The situation for the SSC is quite different, and there is a substantial cost advantage for a two-in-one design. The two adjacent magnets can be rigidly fastened together for simplicity, and alignment of one magnet with respect to the adjacent magent is accurately fixed at assembly. If the lattice is anti-symmetric, i.e., adjacent quadrupole magnets are F-D, adjustments of the position of the quads can be done on one ring without significant effect on the adjacent ring.[2]

The required field quality is not yet established; however, preliminary calculations show that magnet bore diameters as small as 40 to 50 mm, with reasonable conductor placement accuracy, can produce a satisfactory field.[3] The effect of stray fields from one ring on the adjacent ring, or "cross-talk", must be eliminated or corrected. It is possible to have an iron-free, two-in-one magnet with correction coils having reasonable ampere-turn requirements;[4] an advantage of the air-core configuration is the elimination of non-linear iron saturation effects. However, with an iron flux-return, some field enhancement is provided by the iron, cross-talk is reduced, and the iron can be used structurally.

We present some results of a parametric study[5] of two-in-one, iron-core magnets for an SSC. These results are necessarily preliminary in nature, and are intended only to show some of the trade-offs for a wide range of the variables. We show also some results for a reference design that produces 6.5 T in the aperture at 4.4 K for a coil inside diameter of 40 mm. It is not to be inferred that we have established this to be an optimum in any sense.

*This work was supported by the Director, Office of Energy Research, Office of High Energy and Nuclear Physics, High Energy Physics Division, U. S. Dept. of Energy, under Contract No. DE-AC03-76SF00098.

Basis for the Parameter Study

Iron Flux-Return Yoke

To simplify the "real iron" field calculations (we used the POISSON program), we used a scaling method that permitted the results of a single set of real-iron calculations to be used for a variety of coils having various inside and outside diameters, and peak current densities. (Details are presented in Reference 5).

The iron shapes employed in the study are illustrated in Fig. 1. The ones shown in the upper part of Fig. 1 were designed to saturate significantly at aperture fields of 4, 5.5, and 7 T for iron designations I1, I2, and I3, respectively, while those shown in the lower part were used to determine the effects of coil-to-coil spacing; they are identical to configuration I2 except for the spacing. In all cases considered, the iron has a circular hole that fits closely around the coil.

Coil

We used a current density in the coil that varies with azimuth exactly as cosine theta. For the radial variation of current density we used the arithmetic average of the fields produced by two cases: the current density varies inversely with radius in one case, and is uniform in radius in the other case; our experience is that this averaging gives results that are within 5% of those for more realistic coils based on either "cosine theta" or "intersecting ellipse" approximations.

Current Density

We assume that the current density of Nb-46.5 Ti can be significantly improved compared to the specifications used for the Fermilab Doubler magnets, and further, that this improvement can be obtained with an insignificant increase in cost by careful attention to microstructure[6]. Several small batches of high-j_c material have been made by several manufacturers, and the challenge is to obtain this improved behavior in tonnage lots of cable.

As a model, we use the measured j_c of material made several years ago by IMI that has been tested and analyzed by Larbalestier[7]. Using j_c at 5T, 4.2K as a measure for comparison, the Fermilab specifiation is 1850 A/mm^2**; IMI material, 2600 A/mm^2; some material fabricated in China exhibits j_c of 3450 A/mm^2. We use an overall J_c of 0.31 x j_c for the superconductor, which allows for a Cu-to-superconductor ratio of 1.3, and 0.72 for a packing factor and safety factor. Table 1 gives the resulting overall J_c values used in this parameter study. We anticipate improved material to be at least this good in large-scale production after a few years of development efforts.

We have assumed that the ratio of maximum field in the coil to the field in the aperture is 1.08, a figure based on experience with realistic coil designs.

**At $\rho = 5\times10^{-14}$ Ω-m; for $\rho = 10^{-14}$ Ω-m, at which other j_c values in this paper are quoted, j_c will be less by about 5%.

Table 1. Overall maximum current density (A/mm^2) as a function of field, for the indicated temperatures.

Max. field in coil, T	Temperature, K 4.4	1.8
4	870	
5	750	
6	635	
7	520	940
8		830
9		730

Results

In Fig. 2 we show how the iron and coil cross sections vary with aperture field for a coil inside diameter of 40 mm, with operating temperatures of 4.4 and 1.8 K, for iron configurations I1, I2, and I3.

In Table 2 we show the relative cross sections required for the iron and coil for a coil inside diameter of 50 mm as compared with 40 mm.

Table 2. Relative iron and coil cross sections: 5 cm vs. 4 cm coil inside radius

Aperture field (T)	5.0	6.5	8.0
Relative iron cross sec.	1.81	1.27	1.14
Relative coil cross sec.	1.21	1.17	1.12

Temperature, 4.4K
Iron designation, I2

As a point of reference, we adopt a design that gives an aperture field of 6.5 T at 4.4 K for an inside diameter of 40 mm using iron configuration I2.

For this reference design, we show (Fig. 3) how the field aberrations* vary with aperture field. In Tables 3 and 4 we show how the field aberration coefficients vary with iron thickness and coil center-to-center spacing, respectively. (In these tables, the current density is that of the reference design; for the off-design conditions, the aperture field is slightly different from 6.5 T.)

The even-order field-aberration coefficients -- quadrupole, octupole, etc. -- can be caused only by coil-to-coil interactions; for a completely symmetrical magnet they must be exactly zero. The odd-order coefficients are a result of both coil-to-coil interactions and also the iron saturation effects; the latter of might depend on the coil design details.

Discussion of the Results of the Study

Selection of iron thickness

For most of the ring perimeter, the magnitude of the stray field is not of great concern. Thus, in those regions where it is a problem, additional shielding can be placed outside the cryostat. The main function of the iron is not to reduce stray field, but rather to serve as a structural support for the coils, to reduce cross-talk, and to reduce the size of the coil required to produce a particular aperture field value. The minimum iron thickness is determined by structural requirements. Beyond that, an overall cost savings could conceivably be affected by increasing the iron thickness; that would decrease the cost of the coil, but would increase the cost of items associated with the overall size and weight of the magnets -- the iron itself, cryostats, magnet supports, and the refrigeration system. In this study we do not attempt to assess these trade-offs quantitatively.

*We define "multipole coefficients" or "field aberration coefficients", C_n, of the aperture field as the coefficients in the following equations:

$$\begin{vmatrix} B_r \\ B_\theta \end{vmatrix} = \sum_{n=1}^{\infty} C_n \left(\frac{r}{\rho}\right)^{n-1} \begin{vmatrix} \sin(n\theta) \\ \cos(n\theta) \end{vmatrix}$$

"Relative multipole coefficient" is defined as C_n/C_m, m is the number of pole pairs in the magnet, and ρ is an arbitrary reference radius, for which we use 10 mm in this study.

Table 3. Effect of iron thickness on relative multipole coefficients

Multipole order n	Iron designation I1	I2	I3
	Iron leg thickness, mm		
	47.5	60.9	72.5
2	-5.60×10^{-3}	-2.68×10^{-3}	-1.09×10^{-3}
3	$+2.22 \times 10^{-3}$	$+2.80 \times 10^{-3}$	$+3.41 \times 10^{-3}$
4	-4.47×10^{-4}	-2.70×10^{-4}	-1.17×10^{-4}
5	$+7.36 \times 10^{-5}$	$+8.58 \times 10^{-5}$	$+7.78 \times 10^{-5}$
6	-2.66×10^{-5}	-1.70×10^{-6}	-8.90×10^{-6}

Conditions:

Coil inside diameter	= 40 mm
Coil outside diameter	= 72.45 mm
Coil center-to-center spacing	= 130.4 mm
Normalization radius	= 10 mm
Current density	= 521.6 A/sq. mm
Aperture field for iron I2	= 6.5 T

Table 4. Effect of coil center-to-center spacing on relative multipole coefficients.

Multipole order n	Coil center-to-center spacing, mm 86.9	108.7	130.4*	152.2
2	-3.89×10^{-3}	-2.91×10^{-3}	-2.68×10^{-3}	-2.50×10^{-3}
3	$+3.26 \times 10^{-3}$	$+2.93 \times 10^{-3}$	$+2.80 \times 10^{-3}$	$+2.55 \times 10^{-3}$
4	-3.33×10^{-4}	-2.02×10^{-4}	-2.70×10^{-4}	-1.97×10^{-4}
5	$+8.54 \times 10^{-5}$	$+3.39 \times 10^{-5}$	$+8.58 \times 10^{-5}$	$+5.86 \times 10^{-5}$
6	-2.12×10^{-5}	-9.58×10^{-6}	-1.70×10^{-5}	-2.70×10^{-5}

Coil inside diameter	= 40 mm
Coil outside diameter	= 72.45 mm
Normalization radius	= 10 mm
Iron designations	G2,...,J2
Iron leg thickness	= 60.86 mm
Current density	= 521.6 A/sq. mm

Aperture field for coil center-to-center spacing of 130.4 mm = 6.5 T

*Example illustrated in Figs. 4 and 5.

Field aberrations

The systematic quadrupole coefficients are probably not significant; they can be folded into the lattice tuning. The sextupole component can be reduced by clever chopping away of the iron, as demonstrated by G. Morgan[8] at BNL, and then compensated by either active or passive compensation coils[9]. Beyond that, even for a coil inside diameter as small as 40 mm, the relative multipole coefficients are down in the few x 10^{-4} region for any conceivable arrangement, which is probably tolerable. Decreasing the coil-to-coil spacing does not significantly increase cross-talk until the spacing becomes much smaller than that shown in our example designs; mechanical considerations will probably determine the appropriate spacing.

An Example Design

Selection of an optimum field, iron design, and ring-to-ring distance will require consideration of magnet coil and iron costs, cryostat costs, refrigeration costs, compensation-coil requirements, tunnel costs, and so forth, many of which are indeterminable at this time. However, we feel that a design that produces 6.5T with a coil inside diameter of 40 mm is practical and is close to optimum. We have illustrated such a magnet system having the following features. (Fig. 4)

1. Axial position of the magnet is fixed to the cryostat at the midpoint. Longitudinal thermal contraction is accommodated by pivoting of the support rods.
2. The split, laminated-iron yoke is held together by stainless steel keeper bars, which serve to locate the coils precisely during subsequent assembly and also serve to control axial thermal contraction.
3. The magnet can be assembled by first aligning the laminations and welding the inner cryostat in place; the axial keeper bars are part of the inner cryostat wall. Then the magnet, with cryostat inner wall in place, is held in its precisely aligned position while the supports, heat shields, and vacuum enclosure are placed around it; the vacuum enclosure consists of a base, on which all supports are mounted, and a shell that is welded into place after the magnet is mounted and aligned. This assembly technique should minimize alignment problems. After installation the completed magnet is then aligned with reference to the cryostat base.
4. The low-heat-leak supports consist of tension and compression members that can accommodate slight rotation at their ends during cool-down.

Other designs have been examined that have a similar alignment scheme; an example is shown in Fig. 5 which has a compact, re-entrant, sliding, "monopod" support.

We note that, with Nb_3Sn conductor now being developed, a magnet operating at 4.4K with the same coil cross-section as used in the 6.5T example design would produce about 8T.[10] (The iron cross section would of course have to be increased for 8T.)

Fig. 6 shows a similar design for Nb-Ti but for higher field operation at 2K. Superconductor cross section is identical to that of the 6.5 T, 4.4 K design, but more iron is required and the cryostat is more complex.

High field has the obvious advantage of reducing the number of magnets and tunnel perimeter; the cost advantage is large, even after allowing for additional 2 K refrigeration and the more complex cryostat; however, more development is required to verify the practicality of a very extensive 2 K refrigeration system.

Conclusions

Magnet costs are strongly dependent on coil inside diameter, the value of which will probably depend on the field aberration tolerances, and the magnet construction tolerances required to attain them.

Cold iron can be used as a structural support for the coil, reduces cross-talk, and reduces the required amount of superconductor. However, there seems to be no economic incentive to making the iron thicker than what is required to resist the Lorentz forces.

The ring-to-ring spacing will probably not be determined by field-aberration and cross-talk considerations, but rather by mechanical convenience, and possible other factors.

Acknowledgments

The authors express their appreciation to Shlomo Caspi for performing the POISSON calculations, and to Richard Wolgast and Richard Schafer for their contributions to the mechanical design of the cryostat.

References

1. CBA Newletter No. 2, Nov. 1982, Brookhaven National Laboratory.

2. On Improving the Chromatic Effects of Storage Rings with Antisymmetric Insertions, J. Claus et al., IEEE Trans. NS-30, No. 4, p. 2451.

3. Chromatic Properties and Tracking Studies of a 20 TeV pp Collider, A. Garren et al. LBL Report No. 16498 (presented at this conference).

4. Conceptual Magnet Design for an Iron-Free Colliding Beam Accelerator, C.E. Taylor, and R.B. Meuser. LBL Report No. 15158, March 1983; IEEE Trans. NS-30, No. 4, p. 2042.

5. A Parametric Study of Magnets for the SSC, Robert B. Meuser, LBL Engineering Note M6133, Aug. 1983.

6. The Importance of Microstructure in Determining Superconducting Properties, D.C. Larbalestier, A. West, and D.B. Smathers. To be presented at the Int. Conf. on Cryogenic Materials, Aug. 1983, Colorado Springs, Colorado.

7. Superconducting Materials for Particle Accelerator Magnets, D.C. Larbalestier. IEEE Trans. NS-30, No. 4, p. 3299.

8. The Four-Bolt Double Dipole with Shaped Iron for Control of Saturation, G. Morgan. BNL internal report Field Computation Note No. 5, June 8 1982 and subsequent reports.

9. Self-Correction Coil, Operation Mechanism, K. Hosoyama, LBL Report No. 16304, June 1983.

10. Properties and Performance of High-Current-Density Sn-Core Process MF Nb_3Sn, R. E. Schwall, et al., IEEE Trans. MAG-19, No. 3, p. 1135.

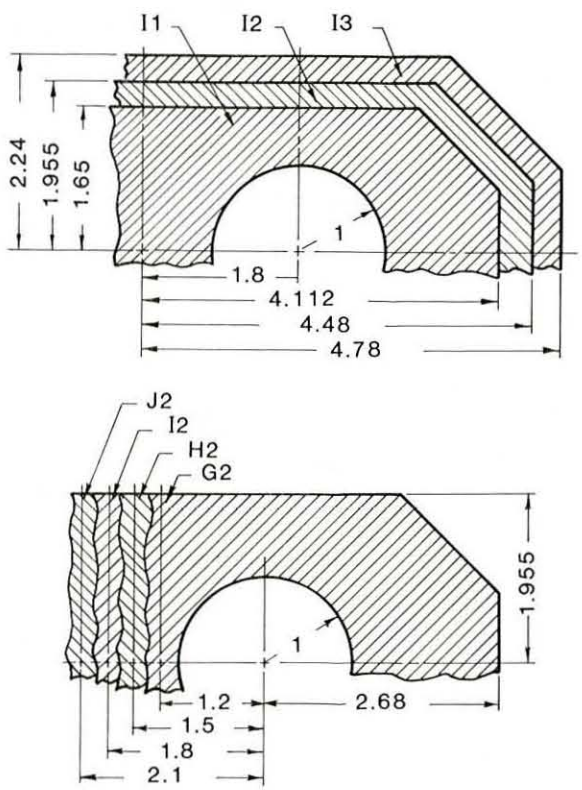

Fig. 1. Iron core configurations employed in the parameter study.

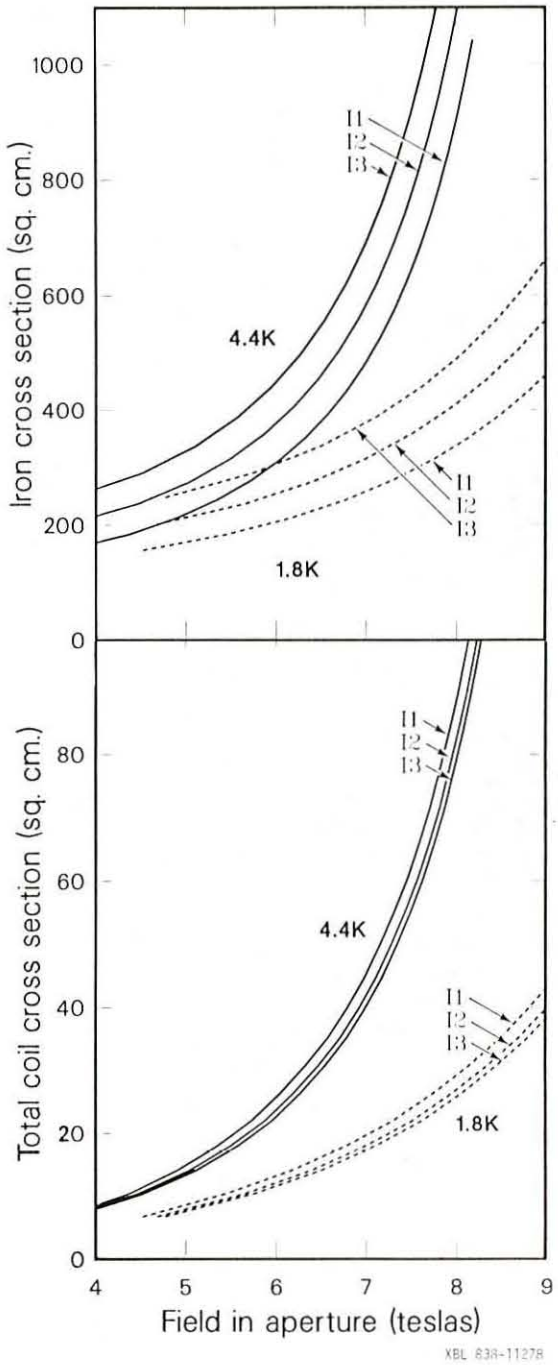

Fig. 2. Required coil and iron cross sections as a function of operating temperature and iron yoke thickness for a coil inside diameter of 4 cm. (Coil cross section is total for both coils.)

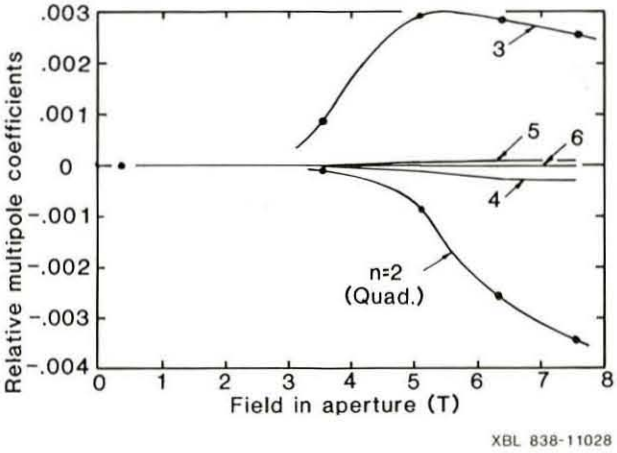

Fig. 3. Variation of field aberration coefficients with aperture field; coil inside diam., 40 mm; temperature, 4.4K; iron designation, I2.

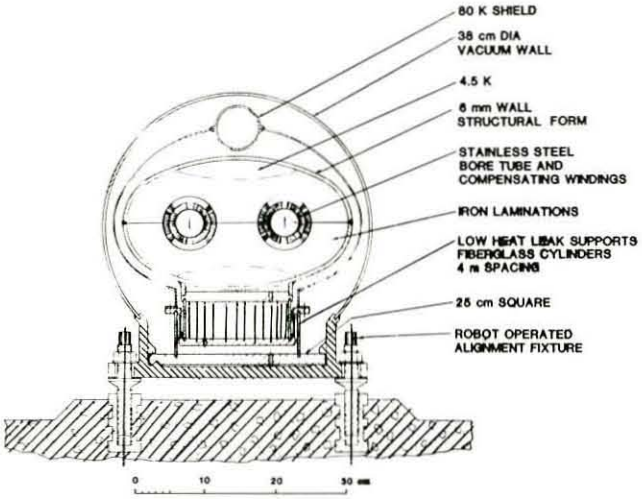

Fig. 5. Cross section of an example design using monopod supports; parameters are the same as those of Fig. 4.

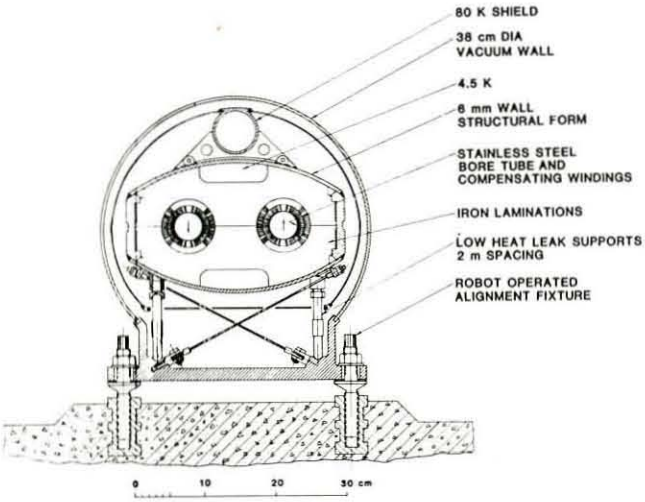

Fig. 4. Cross section of an example design using strut-and-tension-rod supports. Aperture field, 6.5T; coil inside diameter, 4 cm; operating temperature, 4.4K; beam center-line spacing, 13.4 cm; conductor, Nb-Ti.

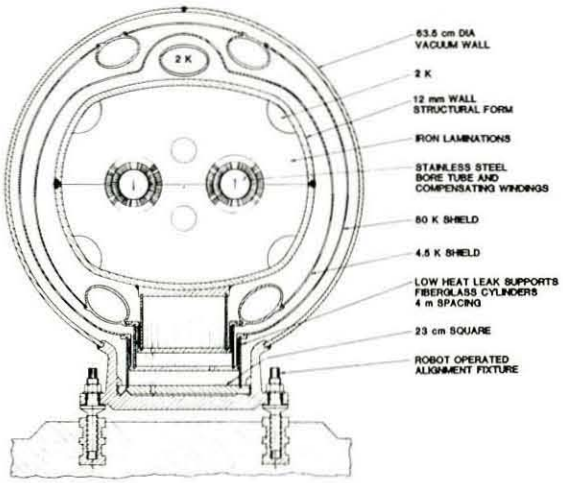

Fig. 6. Cross section of an example design for an aperture field of 8T, using Nb_3Sn conductor. Coil cross section is the same as that of the example shown in Figs. 4 and 5.